Pure and Fe doped TiO$_2$ thin films for MOSFET Technology

Davinder Singh[1*], Alka Singhal[2], Neenu Saini[3]

[1]Department of Physics, Davinder Singh, Pt. JLN Govt. College Faridabad, 121002, India
[2]Department of Physics, Alka Singhal, D.A.V. College For Girls, Yamuna Nagar 135001, India
. [3]Department of Physics, Neenu Saini, Pt. JLN Govt. College Faridabad, 121002, India

*_Corresponding Author: dsingh.singh1973@gmail.com +919467391235_

Abstract **-** Sol-gel dip coating was used to obtain undoped and Fe doped TiO$_2$ thin films deposited on ITO (indium tin oxide) coated glass substrate. These films were sintered at 500°C for 1 hour and were thoroughly characterized with respect to their crystal structure, phase transformation and elemental composition. The structural and dielectric properties of the films were characterized by XPS, TEM, and impedance analyzer. The elemental composition and the oxidation state of the elements in the films were investigated by XPS, titanium peaks were observed at 458.67eV, 457.45eV and 457.28eV that belongs to Ti^{+4}. The presence of Fe^{+3} in the samples is indicated by peaks found at 717.9eV and 709.41eV (2p$_{1/2}$ and 2p$_{3/2}$) state and at 743eV TEM studies confirm mostly the crystallite anatase and rutile phase for the Fe doped TiO$_2$ films. Particle size decreased from 35 nm to 17 nm by 10-mol % iron doping. The density of interfacial states decreases with increase in iron concentration. XPS studies reveal that titanium exists in Ti^{+4} state in all the samples. Dielectric conductivity increased with increase in Fe concentration. Different types of polarization processes exist in different regions of frequency due to which the value of dielectric constant changes in pure as well as Fe doped TiO$_2$ thin films.

Keywords- Sol-gel, anatase, rutile.

I. INTRODUCTION

The need for high permitivity gate insulators for FETs continues to the backbone of the integrated industry. The success of IC largely depends upon near perfection of the SiO$_2$/Si interface. As MOSFET dimensions have scaled, correspondingly larger values of the oxide capacitance have been required. This oxide capacitance is necessary to invert the surface to a sufficient sheet charge density to obtain the desired current (switching) for a given supply voltage and to avoid short channel behavior. Short channel behavior leads to I) increased output conductance in the saturation regime (channel length modulation) II) Increased leakage in the threshold regime (drain induced barrier lowering), and III) A dependence of the threshold voltage (V$_t$) on the channel length. The last two factors are particularly acute problems in the deeply scaled FETs where low supply voltages produce a severe trade off between performance and leakage. Short channel effects that reduce threshold voltage control and increase the threshold slope i.e. increase the leakage current exponentially. Incomplete scaling of the gate oxide control therefore make the manufacture of high density integrated circuits based on sub micron MOSFETS impractical.

The technology road map for semiconductors predicts a direct scaling of the gate oxide thickness while thicker oxides are used in power limited applications and thinner oxides are used in performance driven applications. As the gate oxide thins, however the gate leakage current rises sharply because of direct tunneling between the semiconductor and gate electrode. Minimum acceptable value for the gate leakage is determined by performance and power dissipation concern. The absolute limit is application dependent, the typical absolute limits for physical silicon dioxide thickness is 1.6-2.0 nm. One might therefore consider replacement material for SiO$_2$; particularly extremely thin SiO$_2$ and Nitrided oxides have been used for some time primarily to increase the dielectric diffusion resistance. While the introduction of nitrogen increases the dielectric constant slightly, it also decreases the band gap. Thus only the modest increase in gate oxide capacitance can be achieved for a given leakage current by simple nitrogen incorporation. For simple dielectrics the band gap generally decreases as permittivity increases. Alternatively one can use lattice polarizable materials for the gate insulator. In these materials a high permittivity is obtained by a physical displacement of one or more atoms in a response to an applied electric field. A large increase of dielectric constant however occurs via ionic polarizibility caused by the dipole-

active displacements of chemically bonded ions. An applied electric field induces large ion displacements if a bond has a smaller force constant, indicative of the lower vibrational frequency ("softer" vibrations). Transition metal ions can produce an increased ionic, as well as electronic component of polarizibility because of the presence of open shell d electrons with high anisotropic electronic spatial distributions. Most lattice polarizable materials are metal oxides. For high permittivity materials the GOE (gate oxide equivalent) is typically much less than the physical thickness. As a result it is possible to substantially reduce direct tunneling currents while obtaining the necessary small values of the GOE. For different dielectric materials, the gate current can be obtained by just changing the material parameters such as permittivity, band gap and band offset. The values of band offsets of various high dielectric materials (Al_2O_3, Y_2O_3, La_2O_3, $ZrSiO_4$, SiO_2, $BaZrO_3$, Ta_2O_5, ZrO_2, HFO_2 and TiO_2) are (2.8, 2.3, 2.3, 1.5, 3.5, 0.8, 0.31.4, 1.5 and 0.05) eV respectively and these are now being evaluated as gate dielectrics [1-9].The disadvantage of Y_2O_3, ZrO_2 and other like HFO_2 is that they are fast ion conductors with rather high oxygen ion diffusivity. Conventional materials for MOSFETs were Ge, Si, GaAs and (III-V) compounds. The present research focus is on this category of materials, which include Ta_2O_5, $SrTiO_3$, ZnO and TiO_2. TiO_2 have advantage over other materials because of its high permittivity, better operational condition, lower power dissipation and its acceptance in most modern CMOS (Complementary metal-oxide semiconductor) fabrication facilities. Semiconductor industry scaled the MOSFET channels based on Moore's law.

Typical reported values of dielectric constant for TiO_2 films range from 30 to 100 [10-12]. It is believed that this valadility is related to the presence of low permitivity interfacial layers and to the dependence of permitivity on crystalline phase. Titanium oxide form a number of phases; most common being anatase and rutile. The band gap of the material lies between 3.0 to 3.5 eV, again depending on the crystalline phase. In comparison of TiO_2 and SiO_2 as FET gate insulator comparatively thicker layers of TiO_2 are expected to give same GOE, which prevents direct tunneling between gate and substrate. Leakage current remains a concern as band gap is reduced from approximately 9.0 to 3.0 eV. Studies have suggested that the leakage current at moderate bias can be determined by therminoic emission. So ideally TiO_2 could provide potentially viable approach to dielectrics whose oxide equivalent thickness is less than 2.0 nm. The various properties of TiO_2 suitable for semiconductor technology, such as dielectric constant, dielectric loss, quality factor, and crystallite size etc. can be controlled by preparation technique and control of other parameters. Amongst a variety of transitional metals, iron has been considered to be an appropriate candidate due to the fact that the radius of Fe^{+3} (0.69 nm) is similar to that of Ti^{+4} (0.74nm), so Fe^{+3} can be easily incorporated into crystal lattice of TiO_2 [13]. Titanium alkoxide, titanium (IV) chloride and elemental titanium are most frequently selected precursors for synthesis in which different iron salts (Fe (NO_3), $FeCl_2$, and $FeCl_3$) or other iron compounds (Fe (III) Acac, Fe $(CO)_5$ and ferrocene) were employed. The sol-gel technique, chosen here has utility over other techniques like Physical vapor deposition (PVD), Chemical vapor deposition (CVD), sputtering etc, as it provides stochimeteric film composition and uniform and easy doping for several ions. As it has been reported by various authors in literature that TiO_2 films sintered at $500^\circ C$ have anatase phase. Various metal ion dopants promote the phase transformation from anatase to rutile phase. Iron (Fe) is one of them. The metal ion dopant decreases the optical band gap between conduction band and valance band. The electron densities around the dopant are large in the valance band and small in conduction band as compare to pure TiO_2, which changes the dielectric constant. The aim of this paper is to modify the structural, and dielectric properties of pure TiO_2 films by iron doping for MOSFET applications.

II. EXPERIMENTAL

2.1. Preparation of TiO_2 precursor solution
We started with 0.5M titanium butaoxide solution in isopropyl alcohol. This solution was partially hydrolyzed by adding calculated amount of water while using HNO_3 as catalyst for the hydrolization reaction as reported earlier [14]. The mixture was stirred vigorously with a magnetic stirrer till a clear and transparent sol was obtained. Calculated amount of iron acetyl acetonate compound, dissolved in isopropyl alcohol, was added in the TiO_2 solution to obtain iron doped TiO_2 precursor solution or nano-particles. Iron concentration was varied from 2 to 10 mol% in relation to TiO_2 to have different doping levels. All the chemicals used were of AR grade and were used as procured without further purification.

2.2. Preparation of pure TiO_2 and Fe /TiO_2 films
The ITO/TiO_2/Al hetrostructure was prepared by depositing the TiO_2 on a commercial conducting ITO conducting coated glass substrate and Al top electrode was fabricated by vacuum deposition technique and bottom electrode was fabricated using photolithography technique. The thickness of ITO electrode is 500 nm and that of Al electrode is 300 nm. Al was chosen since it has a low work function of 4.2 eV and should provide an ohmic contact with the TiO_2; which has an electron affinity of around 4.0 eV. The value of work function of ITO is 4.5 eV which is larger than that of Al with TiO_2 is expected to surface defects at the metal surface.
Copper wires were silvered on the top electrode of film and on the ITO bottom electrode for dielectrical measurements. For thin film deposition, the substrates were cleaned in chromic acid followed by rinsing in plenty of de-ionized water and then dried before deposition. The substrates were

dipped in the precursor solution and allowed to settle for two minutes before pulling out at a constant speed to obtain films of 140-160 nm thicknesses. Thin film of TiO_2 that formed on the ITO coated glass substrates were dried in air at room temperature, followed by drying at 100°C for 30 min in an electric oven. The films thus formed were further annealed at 500°C for 1 hr in an electric furnace. Temperature of the furnace was increased at a constant rate of 3°C per minute up to the desired value of 500°C.

Iron doped titania films were prepared from Fe doped TiO_2 precursor solution and processed by the same parameters as that of pure TiO_2 thin films. Iron acetylacetonate [Fe(acac)$_2$] was used as basic material for doping TiO_2 precursor. Addition of iron acetylacetonate yields more homogeneous distribution of iron for each film [15]. For TEM analysis the samples were prepared on copper grid and processed in the same way as that of samples prepared on ITO coated glass. Annealed samples were analyzed by TEM (Transmission Electron Microscopy) model JEOL JEM200CX to get the structure and phase identification in the thin films. Samples were analyzed by XPS for the presence of elements and their compositions. We have studied the dielectric properties of the samples with 4192A IMPEDANCE ANALYZER in the frequency range 100 Hz to 10 MHz.

III. RESULTS AND DISCUSSION

3.1. TEM Studies

TEM images of pure, 6 mol % and 10 mol % iron doped TiO_2 films taken at accelerating voltage of 16 keV, are shown in figure1(a),1(b) and 1(c). The inset in figures shows the electron diffraction spectra of the samples. Polycrystalline growth has been identified in all the samples, the crystallites are randomly oriented and so lattice planes, on the substrate surface. The measured values of d spacing from electron diffraction studies, in the crystallites are listed in table -1. TEM studies reveal the existence of both anatase and rutile phases of TiO_2 in the samples. However brookite phase also found in pure TiO_2 films and in 10 mol% Fe doped TiO_2 films Fe_2O_3 also found corresponding to the planes (511) and (440)
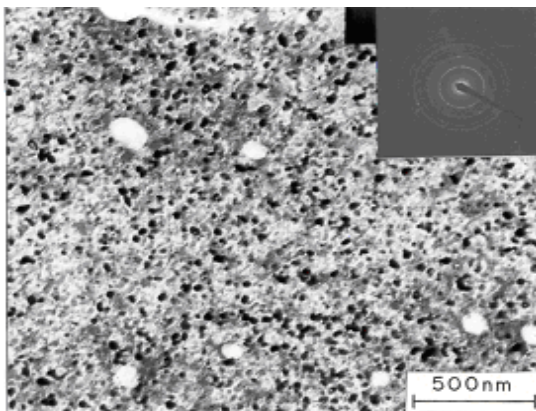

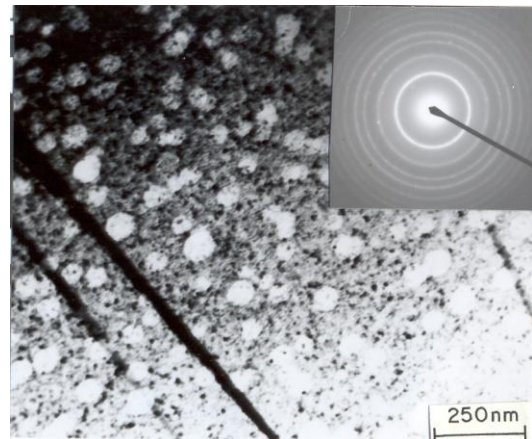Fig.1 (a) TEM image of Pure TiO_2 film

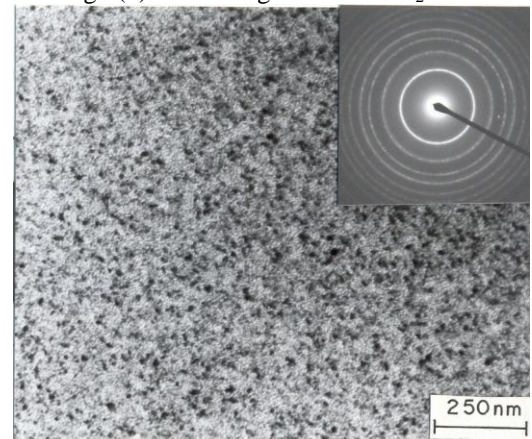Fig.1(b) TEM image of 6 Fe/TiO_2 Film

Fig.1 (c) TEM image of 10 Fe/TiO_2 Film

Particles are spherical in shape in pure and iron doped TiO_2 films. The pores of different diameters are present in all the samples. The average diameter of spherical particle is ~ 35 nm in pure TiO_2 film, while its value is 20 nm and 17 nm for 6 mol % and 10 mol % iron doped TiO_2 films respectively. This indicates a decrease in particle size with increase in Fe doping concentration. The particle size decreased due to change in the surface charge and distance between the particles in the TiO_2 solution. Electron diffraction (ED) patterns have been used for phase identification as shown in insets of Fig. number 1(a), 1(b) and 1(c) respectively. The d spacings for some of the rings were calculated from the formula [16].

$$d = \frac{L\lambda}{r}$$

Where r is the radius of the ring in the diffraction pattern (mm), L is the camera length (the distance between the specimen and the photographic plate, in these observations, it is 1000 mm), λ the wavelength of electron beam (0.0316

Å) at 160 Kev and d is the interplanar spacing of the ring (Å). According to the above formula, the lattice planes spacing's were calculated as listed in the Table 1.

Table number1.

Conc. of Fe	Lattice planes	d spacing (Å)	Phase
Pure TiO$_2$	123	1.541	Brookite
	116	1.359	Anatase
	101	3.420	Anatase
	121	2.872	Brookite
	112	1.685	Anatase
6 mol% Fe/Tio$_2$	210	2.038	Rutile
	200	2.281	Rutile
	107	2.808	Anatase
	105	1.763	Anatase
10 mol% Fe/Tio$_2$	210	2.024	Rutile
	200	2.257	Rutile
	400	2.939	Monoclinic
	511	1.600	Fe$_2$o$_3$
	440	1.487	Fe$_2$o$_3$
	116	1.373	Anatase

3.2. X-Ray Photoelectron Spectroscopy

The photoelectron spectra of pure and iron doped TiO$_2$ films annealed at 500^{0}C for 1 hour is shown in fig nos. 2 (a), 2(b) and 2(c). During the measurements, development of static charge at the sample surface created a problem in locating the actual binding energy positions of Ti 2p and O 1S lines. To overcome this problem the amount of static charge was also determined by keeping the binding energy positions of C1S line fixed at 284.6 eV. [17]. Thus the amount of static charge that develops on the film surface was also estimated to be 1.3 eV. In the present study, the actual binding energy positions corresponding to Ti 2p$_{3/2}$ and Ti 2p$_{½}$ lines for pure TiO$_2$ films were found at 457.95 and 463.6 eV, these indicate the presence of Ti^{+4} in TiO$_2$ films [18]. Titanium was also in the Ti^{+4} state in all the iron doped TiO$_2$ films.
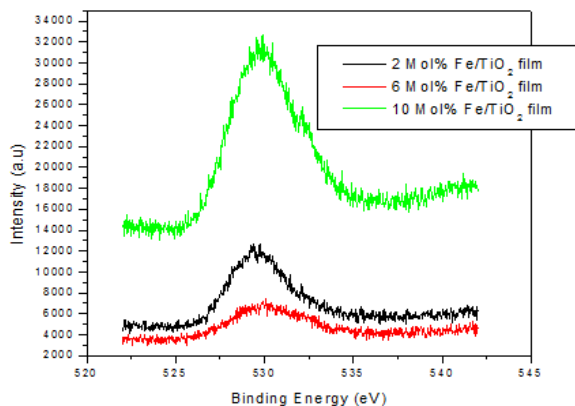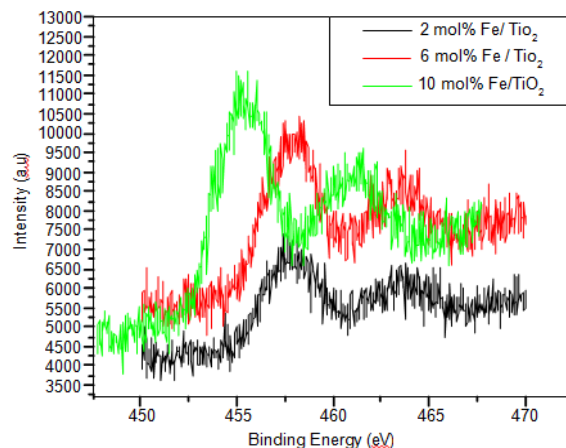

Fig. 2(a)

Fig. 2(b)

X-ray photoelectron spectroscopy was also used to reveal the state of iron in the samples. This technique is suitable for determining the titanium-iron ratio in the samples in the top 1-2 nm layer of particles.
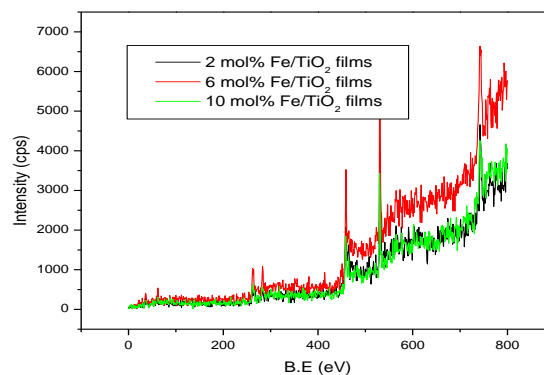

Fig. 2(c). XPS spectra of Pure and Fe doped TiO$_2$ films

Three samples were investigated: TiO$_2$-2Fe, TiO$_2$-6 Fe and TiO$_2$ -10 Fe. The presence of Fe^{+3} in the samples is clearly indicated by peaks found at 717.9 eV and 709.41 eV (2p$_{1/2}$ and 2p$_{3/2}$) state and at 743 eV state.

Titanium peaks were found at 458.67 eV, 457.45 eV and 457.28 eV that belongs to Ti^{+4}. The presence of Ti^{+3}cannot be confirmed from these experiments. The higher concentration of Fe indicates that during the synthesis a certain amount of dopant is accumulated in the surface layer.

3.3. Dielectric studies:
Dielectric constant
Typically, electronic polarization persists until a frequency of about 10^{16} Hz, atomic polarization until about 10^{13} Hz, while the dispersion for orientational polarization may lie anywhere within a wide frequency range, say 10^2 to 10^{10} Hz,

depending on the material and its temperature. In addition to these polarizations mechanisms the existence of interfacial effects such as macroscopic discontinuities in the material, or blocking at the electrodes, causes the trapping of charge carriers, and such phenomena, as well as inclusion in the dielectric of impurities giving rise to conducting regions.

Dielectric constant (ε) has been calculated by measuring the capacitance (C), between the two electrodes by simple relationship

$$\varepsilon = \frac{C_m}{C_0}$$

Where C_m is the measured value of capacitance and C_0 is the value of capacitance of the structure in absence of TiO$_2$ film.
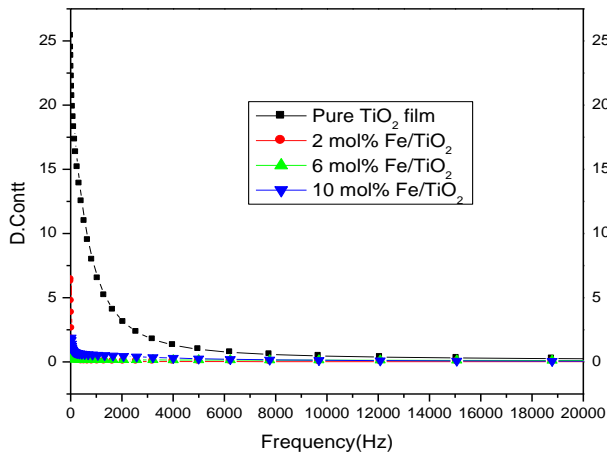

Fig. 3 Dielectric Constant Vs Frequency

Fig.3 shows the room temperature frequency dependence dielectric constant (ε) spectra of iron doped TiO$_2$ films. A decrease in the value of dielectric constant with increase in frequency has been observed (figure no.3). These curves closely resemble those predicted by Debey relaxation model for orientational polarization. With more than 8 mol% iron doping the value of dielectric constant goes less than 1. The change is well pronounced for in undoped and the samples having low doping levels. The major change takes place in the very low frequency region (~ 20 -70 Hz). Such behavior at very low frequency is expected due to the interfacial polarization, where charge carriers, migrated under the influence of an electric field are thought to be blocked at the electrode dielectric interface. The value of dielectric constant decreases with increase in Fe content and due to decrease in   particle size. These curves closely resemble those predicted by the Debye relaxation model for orientational polarization [19].   Recently dielectric properties of TiO$_2$ in various systems have been studied, including DC magnetron-sputtered TiO$_2$ thin films for MIM

structures (Al/TiO$_2$/Al and MIS structures (Al/anataseTiO$_2$/Si), (Al/amorphous TiO$_2$/Si), and RF magnetron sputtered (Al/rutile TiO$_2$/Si). However, there is some discrepancy in the values of dielectric constant recorder for TiO$_2$ thin film. Indeed ε ~ 60 has been recorded in relatively thick (~600 nm) anatase TiO$_2$ films at V< 80 KV/cm and ε ~ 200 at V> 200 kV/cm and at frequency 1 KHz. The dielectric constant of amorphous TiO$_2$ thin films have been recorded ε ~ 73 for thickness 200 nm, ε~13.7 for thickness 94 nm, and ε~18.4 for 105 nm.. It is generally accepted that the dielectric constant of rutile phase is higher than that of anatase. ; However this is not necessary true [20]. The discrepancies may be explained assuming that such experimental parameters as film thickness, frequency of measurements, the magnitude of applied electric field and temperature may affect the dielectric constant.

D. Loss

Fig. 4 shows the d. loss of Fe doped samples. In case of 10-mol % Fe doped the value of d.loss is smallest in comparison to the other doped samples. In low frequency range, when the electrical dipoles are able to follow the variation of electric field dielectric loss decreases with increases of signal frequency and then becomes constant except 10 mol % Fe doped TiO$_2$ film.
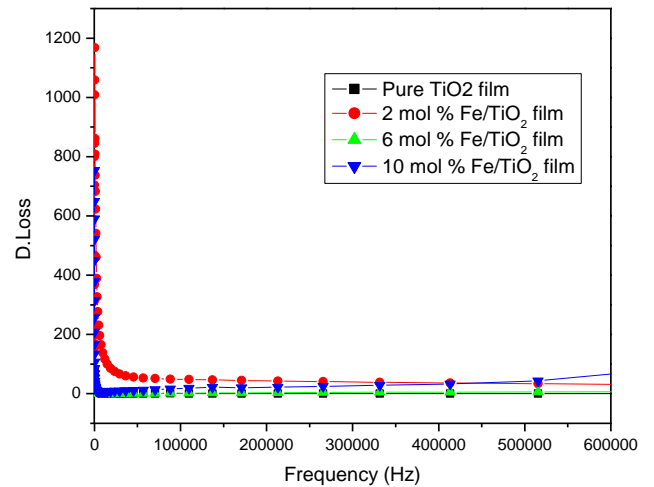

Fig.4 Dielectric loss of Fe doped TiO$_2$ films.

The increase loss factor with decreasing frequency is usually associated with ion drift, dipole polarization or interfacial polarization [21-22]. For high permittivity the GOE is typically much less than the physical thickness as a result it reduces the direct tunneling current while obtaining the necessary small values of GOE. In these samples (pure and iron doped) the values of GOE are 14 nm, 67 nm, 210 nm 381 nm for pure, 2 mol%, 6 mol% and 10-mol% iron doped TiO$_2$ films. The iron doping increases the d.loss

(conductivity) for such an extent that samples do not exhibit intrinsic dielectric response.

Dielectric conductivity

The log σ versus log frequency plots at different concentration of iron are shown in fig. no.5. The conductivity curves exhibit two different regions. The low frequency region and high frequency region. At low frequencies, a plateau which characterizes the direct current Conduction is present, while at higher frequencies the conductivity increases gradually with the frequency. The AC conductivity of the Fe doped TiO_2 films exhibits the universal power law behavior

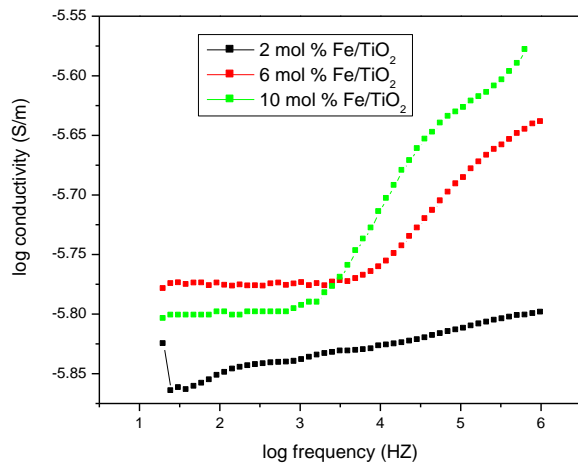$$\sigma = \sigma_{dc} + A\omega^s \quad (1)$$

Fig.5 Log conductivity Versus Log Frequency

Where σ_{dc} is the DC conductivity, and s and A are the characteristic parameters, s is the exponent of the power law, besides 0<s<1. This exponent is used to characterize the electrical conduction mechanisms in different materials. It is indicative of interactions between all the charge species participating in the polarization process. The value of the frequency exponent (s) is determined by taking the log of equation (1)

$$S = \frac{d \log \sigma}{d \log f}$$

It is clear from the fig.6 that according to relation $\sigma \propto f^s$ the value of s are .0015, .0024, .0053 and .0054 for pure, 2 , 6 and 10 mol% Fe doped TiO_2 films

Capacitance

It is found that capacitance decreases as the frequency is increased. The larger increase in capacitance towards the lower frequency region can be approximately explained on the basis of charge carriers being blocked at the electrodes, which leads to trap charge layer resulting in the increase in

capacitance [23]. The decreasing behavior of capacitance with the frequency suggests a contribution to the junction space charge from relatively slow deep level states at or near the interface [24].

The total number of interface states (NIS) due to depletion and interface can be calculated from the capacitance measured at low frequency while the capacitance at higher frequency is associated with depletion only. A lower limit of interface states can be calculated from the relation [25]

$$N_{IS} = \frac{C_{LF} - C_{HF}}{e}$$

Where C_{LF} and C_{HF} are the capacitance at low frequency 20 Hz and high frequency 213166 Hz respectively. The total number of interface states, which is responsible for the dispersion of capacitance was found to be increasing with increase in concentration of iron as given in table no. 2

Table no. 2

Conc. Of iron	Total no of interfacial states 10^{11} $(cm^{-2} eV^{-1})$
PureTiO$_2$	4.562
2-mol %	2.167
6-mol %	0.618
10–mol %	0.474

IV. CONCLUSIONS

High dielectric constant pure and iron doped TiO_2 films have been fabricated by means of an optimized sol-gel process. TEM studies revealed that particle size decreases with increase in iron concentration. The number of interfacial states decreased with increase in iron concentration. XPS shows that Ti exists in Ti^{+4} state in pure as well as iron-doped samples. The density of sates decreased with increase in iron concentration, which suggests that leakage current density decreases. Dielectric constant decreased with increase in iron concentration and with frequency. The decrease in dielectric constant is due to decrease in particle size and grain boundary surface area. From these results (high dielectric constant, low leakage current, less number of interfacial states, high break down strength and low band offset) of TiO_2 films suggests that it is a promising candidate of high k gate dielectrics. The manufacturing cost of TiO_2 based FET can be lower utilizing the low cost material and simple processing.

working as scientist in NPL New Delhi for their help in characterization of the samples.

REFERENCES

[1]. G. D Wilk., R. M. Wallace., J. M. Anthony., Journal of Applied Physics, Vol. **89**, pp. **5243, 2001.**

[2]. G. D Wilk., W. L. Gladfelter; IEEE Tras. ED, Vol. **44**, pp. **104, 1997**.

[3]. L. Manchanda., et al., Tech. Dig. IEDM, pp. **605, 1998**.

[4]. E. P. Gusev., M. Copel., E. Cartier., I. J. R.Baumuol., C. Krug., M. A. Gribelyuk., Appl. Phys. lett.
Vol. **76**, pp. **176, 2000.**

[5]. G. B. Alers., et al , Applied Physics., Letters, Vol. **73**, issue.11, pp. **1517**, **1998**.

[6]. M. Copel., M. Gribelyuk., E. Gusev., Applied Physics Letters, Vol. **76**, pp. **436, 2000.**

[7]. Y. H.Wu., M. Y.Yang., A.Chin., W. J. Chen., C. M. Kwei., IEEE Electron Device Letters, Vol. **21**, pp. **341, 2000.**

[8]. J. Kwo., et al ., Journal Applied Physics, Vol. **89**, pp**. 3920, 2001.**

[9]. H. J.Osten., J. P. Liu., P.Gaworzewski., E. Buigel., P. Zaumseil., Tech. Digest IEDM, 28.5.1 (2000)

[10]. J. Hang., J. S. Yuan., Y Ma., A. S.Oater., Solid State Electron, Vol. **44**, pp. **2165**, **2000.**

[11]. M. D. Stamate., Thin Solid Films, Vol. **372**, pp**. 246**, **2000.**

[12]. A. Shibata., Japan Journal of Applied Physics, Vol. **30**, **L650 1991.**

[13]. W.Choi., A.Termin., M. R. Hoffman., Journal of Physical Chemistry, Vol. **98,** No. **51,** pp**. 13669-13679, 1994.**

[14]. S.D.Sharama., Davinder Singh., K.K Saini., C.Kant., V. Sharama.,S.C.Jain., C.P.Sharma., Applied Catalysis A, Vol.**40,** pp**. 314, 2006.**

[15]. J. A. Navio., Gerardo Colon., M.Macias., M. I. Litter., Applied Catalysis A, General Vol.**177**, pp.**111**, **1999.**

[16]. T. B. Ryer., Electron Dffraction, Bulter and Tanner., London, pp. **75-78, 1970.**

[17]. P.Swift., D.Shuttleworth., M.P. Shea.,(Eds.) practical surface analyzed by Auger and wiley, London., p**p. 477, 1983.**

[18]. J. Pauilleau., Devilliers., H. Groul., Journal of Material Science, Vol. **32**, pp**. 5645, 1997.**

[19]. H. Birey., Journal of Applied Physics, Vol. **49,** pp. **2898, 1978**.

[20]. M. D. Stamate., Applied Surface Science, Vol. **218**, pp.318, **2003.**

[21]. F. Argal., and A.K. Jouscher., Thin Solid Films Vol. **2**, pp. **185**, **1969.**

[22]. A.Von Hipple., E. P.Gross., F. G. Telstis., A. Geller., Phys. Rev Vol. **91**, pp.**568**, **1953.**

[23]. C. J. Ridge., P. J. Harrop., D. S. Champbell., Thin Solid Films, Vol. **2**, pp. **413, 1968.**

[24]. V.P Singh., H. Brafman., J.Makwana., Sol. Cells, Vol.**31**, pp. **23**, **1993**.

[25]. H. Tavakolian., J.R. Sites., Proceedings of the 20th IEEE Photovoltaic Specialists
Conference, Lasvegas, NV, IEEE, New York, .**1608, 1988.**